Assessment of turbulence models for a wing-in-junction flow

J.L. Coombs[1], C.J. Doolan[1], D.J Moreau[1], A.C. Zander[1], and L.A. Brooks[2]

[1]School of Mechanical Engineering
University of Adelaide, Adelaide, South Australia, 5005, Australia

[2]Deep Blue Tech Pty Ltd
Osborne, South Australia, 5017, Australia

Abstract

The numerous engineering applications involving wing-in-junction-flows makes knowledge of the predictive effectiveness of turbulence models for such flows valuable. The performance of eight turbulence models was assessed for a wing-in-junction flow test case using incompressible Reynolds-averaged Navier-Stokes (RANS) simulations. The case geometry consisted of an airfoil with a 3:2 elliptical leading edge, attached at the point of maximum thickness to a NACA 0020 series tail, mounted on a flat plate. The numerical results for pressure, velocity and turbulent kinetic energy achieved using the various turbulence models were evaluated by comparison with experimental measurements published in the literature. It was found that the Realisable k-ε model, and second-moment closure models, produced the closest agreement to the experimental data.

Introduction

Wing-in-junction-flows occur in many engineering applications where wing-like shapes are attached to a fuselage or hull. It is important to be able to accurately model these flows in order to evaluate the fluid dynamic loading and radiated noise during the design process. Turbulence modelling is an essential part of the flow computation; however, each turbulence model is unique, as each has been developed for a particular flow situation. Hence it is necessary that the most suitable turbulence model be found for the simulation of wing-in-junction flows to assist those who need to analyse and design devices that incorporate them. To this end, the present paper compares the predictive performance of several turbulence models, for a semi-infinite junction flow at Reynolds number based on wing thickness (Re_t) and bulk velocity of $Re_t = 1.15 \times 10^5$. This test case was experimentally investigated by Devenport and Simpson [3]. The extensive experimental measurements available, including detailed inlet flow conditions, as well as geometric simplicity, make reproduction of this experiment an attractive case for investigating the performance of turbulence models, with pressure measurements taken at a variety of locations on the wing as well as the flat plate, as well as multi-component mean and fluctuating velocity measurements in the upstream symmetry plane as well as a variety of cross-steam planes. As a result of this, there have been many computational investigations of turbulence models undertaken for this case, comparing the results not only between each other, but also with the experimental results [1-4,8]. The Apsley and Leschziner [1] study compared over a dozen models, the models investigated predicted the location of the region of lowest pressure coefficient on the plane surface to be upstream of, rather than at, the maximum thickness location of the wing as found in the experimental results. Work to date has had trouble correctly predicting the intensity and location of the point of maximum turbulent kinetic energy in the upstream symmetry plane and the performance of turbulence models, including several yet to be applied to this case before, in predicting this feature will be investigated.

Turbulence models

Eight turbulence models were selected for investigation, the standard k-ε [7], Realisable k-ε [10], Renormalisation Group Theory (RNG) k-ε [13], the 1998 revision of the standard k-ω [12], k-ω SST [8], Launder-Reece-Rodi (LRR) [6], Launder-Gibson [5], and Spalart-Allmaras [11] models. Many of these models performance have previously been investigated, and comparison to those results can be used for validation, however to the authors' knowledge the RNG k-ε, Realisable k-ε, LRR and Launder Gibson models have yet to be applied to this test case, and the evaluation of their performance represents an extension to the current knowledge base.

Geometry and boundary conditions

The case geometry is a 'Rood' wing (a 3:2 elliptical nose connected at the thickest point, of thickness T, to a NACA 0020 tail) attached to a flat plate bottom wall, as shown, with a Cartesian coordinate system, with origin at the wing-plate interface, in Figure 1.
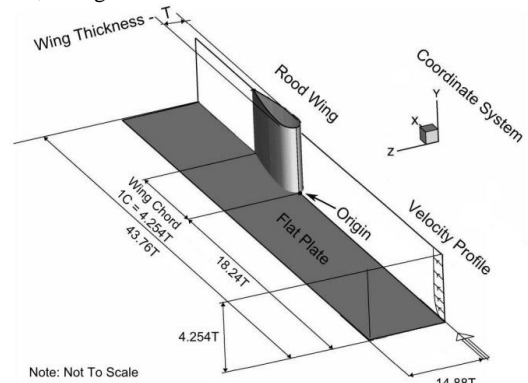

Figure 1. Case geometry and coordinate system, in terms of maximum wing thickness, T.

The five boundaries on this domain are the solid surface formed by the wing-plate, the symmetry plane in the X-Y plane at Z=0, the outlet which consists of the Y-Z plane at X=25.52T as well as the Y-X plane at Z=14.88T, the top plane at Y=4.25T in the X-Z plane, and the inlet at X=-18.24T in the Y-Z plane.

The inlet velocity profile was matched to the experimental data from the literature at the same upstream location. Inlet turbulence properties were specified as uniform values throughout the boundary layer, calculated using a turbulence intensity, I, of 0.2% [1], and an assumed turbulent to molecular viscosity ratio of 1.

The top plane had slip boundary condition applied to it while the wing-plate pair was given a no-slip condition. The symmetry plane had a symmetry plane condition applied. The condition applied on the outlet was a zero-gradient condition.

Meshing and Numerical methods

Steady RANS solutions were obtained using OpenFoam™. Five meshes of increasing resolution in all directions were used, with total cells as given by Table 1. For each mesh, the solution was run until all residuals reached a level of 1×10^{-7} or smaller. The maximum pressure coefficient on the wing surface changed by 0.157% between the realisable k-ε model fine and very fine mesh solutions. This demonstrates that grid convergence was achieved. Wall functions were used throughout.

Mesh level	Total number of cells
Very Coarse	6.35×10^5
Coarse	8.93×10^5
Moderate	1.75×10^6
Fine	2.94×10^6
Very Fine	4.64×10^6

Table 1. Mesh refinement level name and cell count.

Results and discussion

Pressure Coefficient

The pressure coefficient on the wing was compared with that of the literature [2] for all models along the Y/T=0.13279 plane. Figure 2 shows both the experimental results, as well as those for the very fine mesh solution using the Realisable k-ε model.
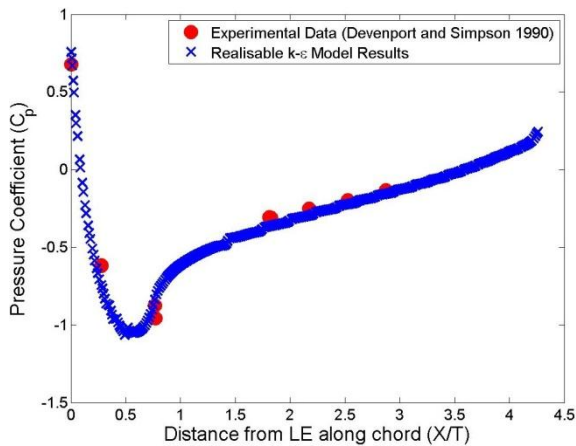

Figure 2. Y/T=0.13279 plane comparison of the very fine mesh Realisable k-ε model solution and experimental [3] wing pressure coefficient.

By interpolation of the simulation results at identical locations to the experimental results, it is possible to quantify the error E of each model according to

$$E = \sum_{i=1}^{n} | C_{pS}^{i} - C_{pE}^{i} |, \tag{1}$$

where n is the total number of points i at which the experimental pressure coefficient, C_{pE}^{i}, is compared to that of the simulation, C_{pS}^{i}. The superscript refers to the value at point i. The calculated error for the very fine mesh solutions for each of the turbulence model is given in Table 2. The ε-based models outperform the ω-based models as well as the Spalart-Allmaras model, with the Realisable k-ε performing best. The majority of the error can be attributed to that all of the models predict the point of lowest pressure coefficient to be further forward than the experimental [3] results.

The pressure coefficient on the flat plate around the wing was calculated and compared with experimental data [3]. The very fine mesh Realisable k-ε solution is shown in Figure 3. The simulation slightly underestimates the minimum pressure coefficient value, and as with the wing pressure coefficient already discussed, similar to the results of other numerical investigations, it locates the minimum pressure coefficient further upstream, rather than at the point of maximum wing thickness. However the simulation is otherwise in good agreement with the experimental results.

Pressure coefficient error for very fine mesh solutions	
Model error	**Error, E**
Realisable k-ε	0.0705
RNG k-ε	0.0711
k-ε	0.0727
Launder-Gibson	0.0727
LRR	0.073
k-ω SST	0.0755
k-ω	0.0771
Spalart-Allmaras	0.0916

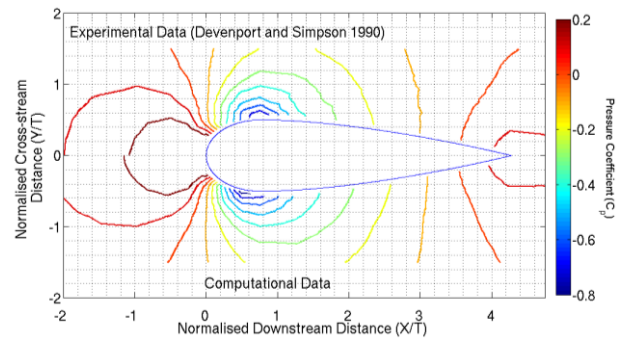Table 2. Model pressure coefficient error.

Figure 3. Comparison of simulated and experimental pressure coefficient data on the flat plate surrounding the airfoil junction.

Upstream Separation

Figure 4 shows the location of planes, defined in the literature [3] as Planes 05 and 10, as well as the symmetry plane, at which comparisons of the velocity components as well as turbulent kinetic energy (k) will be compared. Plane 05 corresponds to the maximum thickness plane of the wing while Plane 10 is one-twentieth of a chord downstream of the trailing edge.
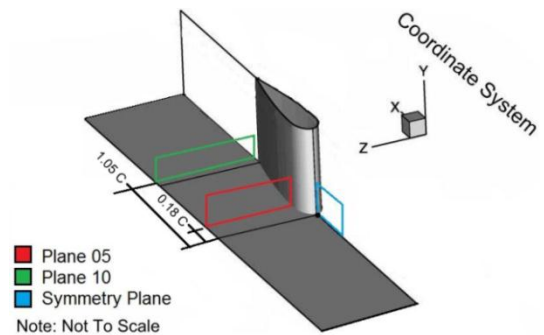

Figure 4. Location of experimental sample planes of interest.

The experimental upstream symmetry plane velocity is shown as a vector plot in Figure 5, as normalised by the freestream velocity, U_{ref}, of 27m/s. As the flow approaches the wing it separates at X/T=-0.38919 and recirculates. Figure 6 shows the Realisable k-ε model solution for the upstream symmetry plane velocity field, which has significantly reduced recirculating flow. The reduced intensity recirculating flow does not extend as far upstream as in the experiment, and results in a separation point closer to the wing.

From interpolation of the experimental [3] and the very fine mesh solutions simulation results, the respective separation points can be found and are given in Table 3. The separation point is strongly linked to viscous effects and turbulent flow, and hence is a sensitive parameter to use for turbulence model assessment.

The results shown do not provide a strong differentiation between the performance of the ε- based and ω-based models, however the simulated results do tend to place the separation point too close to the leading edge of the wing, due to under-predicting the extent and intensity of the return flow, especially the Spalart-Allmaras model, which shows the greatest discrepancy with the experimental [3] results.
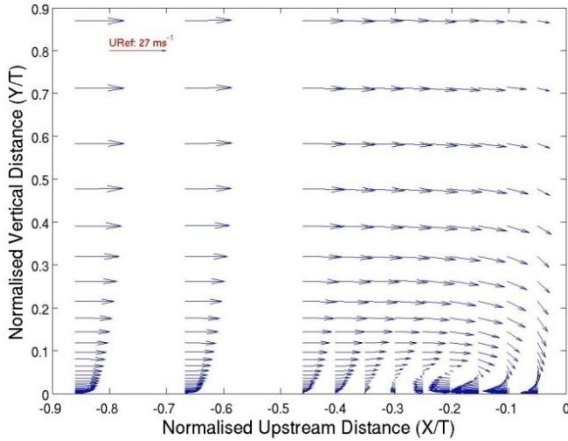

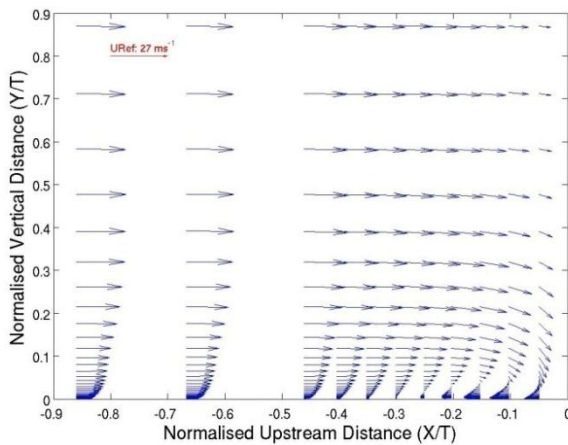Figure 5. Experimental [3] upstream velocity vector plot.

Figure 6. Realisable k-ε model upstream velocity vector plot.

Separation point location for very fine mesh solutions		
Source data	**Separation point location [X/T]**	**Error relative to experimental**
Experimental [3]	-0.38919	0%
Spalart-Allmaras	-0.17726	-54.4541%
k-ε	-0.28407	-27.0099%
LRR	-0.31364	-19.4121%
Realisable k-ε	-0.32994	-15.2239%
k-ω	-0.33234	-14.6073%
Launder-Gibson	-0.40616	4.3603%
RNG k-ε	-0.42634	9.5455%
k-ω SST	-0.4814	23.6928%

Table 3. Separation point location.

Turbulent Kinetic Energy

The turbulent kinetic energy in the upstream symmetry plane was also compared, and Figures 7 and 8 show the experimental [3] and simulated results for the most refined mesh solution using the Realisable k-ε model, respectively. The Realisable k-ε model had the best qualitative agreement with the experimental [3] results of all the models investigated, having the same contour shape and structure, as well as among the best quantitative agreement, with

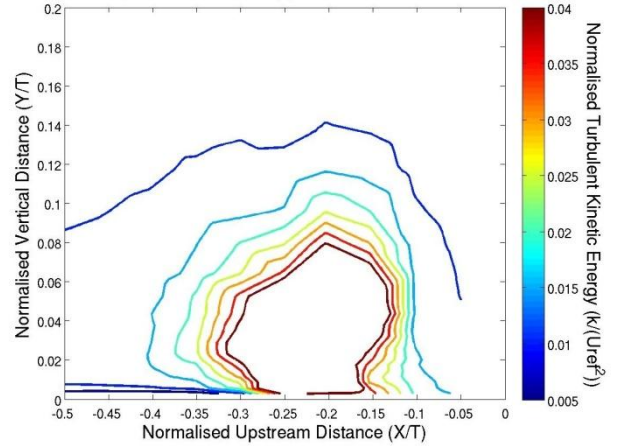the second lowest under-prediction of the turbulent kinetic energy intensity.

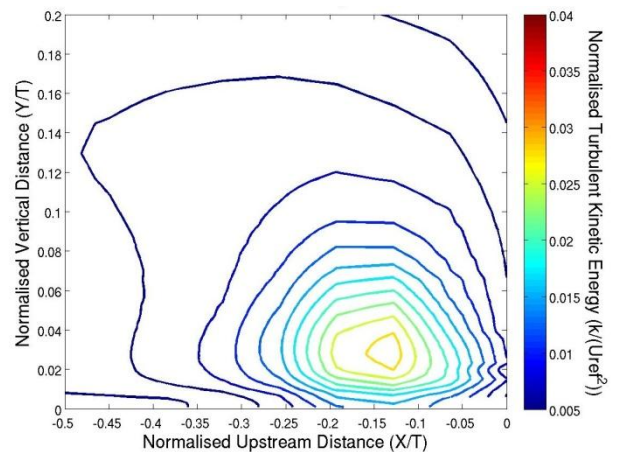Figure 7. Experimental [3] upstream turbulent kinetic energy plot.

Figure 8. Realisable k-ε model upstream turbulent kinetic energy plot.

The location and magnitude of the point of maximum kinetic energy is representative of the models accuracy in predicting the position and intensity of the centre of the recirculation region. Figure 9 provides comparison of the performance of the models in predicting both these quantities, by comparing the distance between the simulated and experimental point of maximum turbulent kinetic energy, R, as well as the ratio of maximum simulated to maximum experimental [3] turbulent kinetic energy. As can be seen from the figure, aside from the k-ω model all the models significantly under-predict the intensity of the turbulent kinetic energy. As for the position of the maximum point, the figure shows that the Reynolds stress models perform best, while the ε-based models outperform the ω-based models.
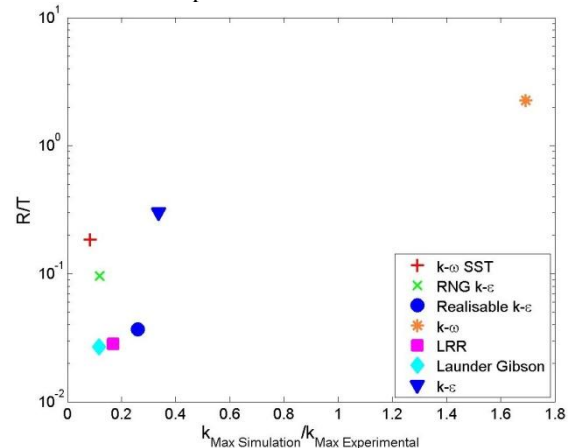

Figure 9. Turbulent kinetic energy performance plot.

In Planes 05 and 10, the vertical velocity component proved the best at differentiating the performance of the models. Figures 10 and 11 show the experimental [3] and simulated vertical velocity contour plots for the finest mesh Realisable *k-ε* solution for Plane 05. It can be seen that the simulation is qualitatively good, appearing to capture the structure far from the wing well, but quantitatively, has significantly reduced near wing flow vertical velocity. The under-prediction of the down-flow in Plane 05 is not repeated in Plane 10, where instead, the simulation again seems to capture the general contour shape well, but in the near all region, it over-predicts the experimentally measured vertical velocity.
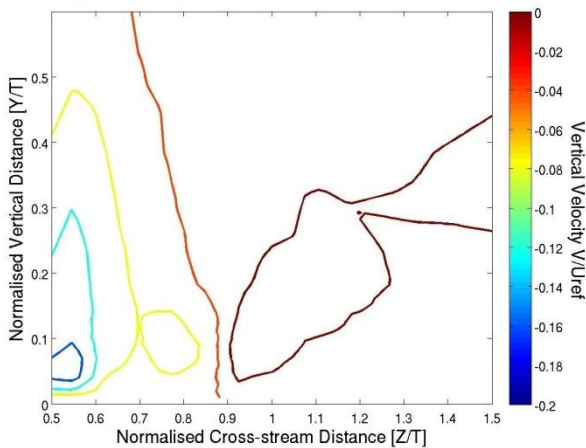

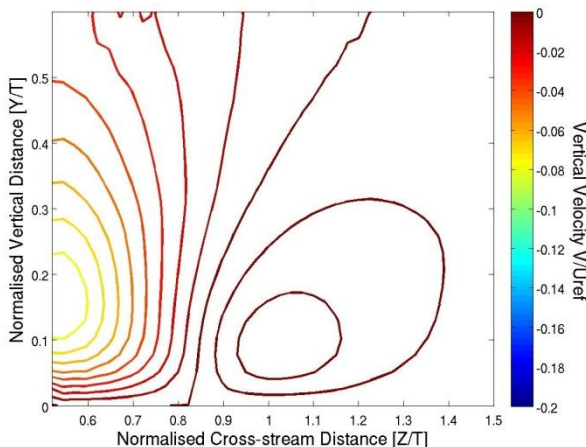Figure 10. Experimental Plane 05 vertical velocity contour plot.

Figure 11. Realisable *k-ε* model upstream Plane 05 vertical velocity contour plot.

Conclusions

Results of a study of turbulence model performance in a junction flow have been presented. Insight into the relative performance of some of the most popular RANS models in junction flows has been provided. For the models which, to the authors knowledge, had not been used on this case before, the results were compared with those of the other models and experiment. Both the LRR and Launder-Gibson models showed better predictive results than most of the simpler one and two equation models, except for the Realisable *k-ε* model. Aside from the *k-ω* SST model, which is known to be overly sensitive [1], in the upstream symmetry plane, none of the models captured the intensity of the return flow, resulting in smaller, less intense recirculation regions, as well as resulting turbulent kinetic energy. This reduction in turbulent kinetic energy relative to the experiment continued, although in decreasing extent, further downstream throughout the domain, in Planes 05 and 10, though all models still significantly under-predict the turbulent kinetic energy measured in the experiment.

References

[1] Apsley, D.D. & Leschziner, M.A., Investigation of advanced turbulence models for the flow in a generic wing-body junction, *Flow, Turbulence and Combustion*, **67**, 2001, 25-55

[2] Chen, H.C., Assessment of a Reynolds stress closure model for appendage-hull junction flows, *Journal of Fluids Engineering*, **117**, 1995, 557-563

[3] Devenport, W.J. & Simpson, R.L., Time-dependent and time-averaged turbulence structure near the nose of a wing-body junction, *Journal of Fluid Mechanics*, **210**, 1990, 23-55.

[4] Fu, S., Xiao, Z., Chen, H., Zhang, Y. & Huang, J., Simulation of wing-body junction flows with hybrid RANS/LES methods, *International Journal of Heat and Fluid Flow*, **28**, 2007, 1379-1390

[5] Gibson, M.M. & Launder, B.E., Ground effects on pressure fluctuations in the atmospheric boundary layer, *Journal of Fluid Mechanics*, **86**, 1978, 491-511.

[6] Launder, B.E., Reece, G.J. & Rodi, W., Progress in the development of a Reynolds-stress turbulence closure, *Journal of Fluid Mechanics*, **68**(3), 1975, 537-566.

[7] Launder, B.E. & Sharma, B.I., Application of the energy-dissipation model of turbulence to the calculation of flow near a spinning disc, *Letters in Heat and Mass Transfer*, **1**, 1974, 131-138.

[8] Menter, F.R., Two-equation eddy-viscosity turbulence models for engineering applications, *AIAA*, **32**, 1994, 1598-1605.

[9] Paciorri, R., Figlioli, A., Mascio, A.D. & Favini, B., RANS simulations of a junction flow, *International Journal of Computational Fluid Dynamics*, **19**(2), 2005, 179-189.

[10] Shih, T.H., Liou, W.W., Shabbir, A., Yang, Z. & Zhu, J., A new k-ε eddy viscosity model for high Reynolds number turbulent flows, *Computers and Fluids*, **24**, 1995, 227-238.

[11] Spalart, P. R. & Allmaras, S. R., A one-equation turbulence model for aerodynamic flows, *Recherche Aerospatiale*, **1**, 1994, 5-21.

[12] Wilcox, D., *Turbulence Modeling for CFD*, DCW Industries Inc., 1998.

[13] Yakhot, V., Orszag, S.A., Thangam, S., Gatski, T.B. & Speziale, C.G., Development of turbulence models for shear flows by a double expansion technique, *Physics of Fluids*, **4**, 1992, 1510-1515.